Enhancing cold retention in small refrigerators using phase change materials: numerical study and thermal modeling

Abdeslem Dhilou[1*], *Mohamed* Errebii[1], *Mustapha* El Alami[1], and *Ayoub* Gounni[1]

[1]LPMAT Laboratory, Department of Physics, FSAC, Hassan II University of Casablanca, Morocco

Abstract. Small refrigerators, active coolers and portable thermal containers are widely used for transporting food products, temperature-sensitive medicines and biological samples. Unfortunately, their thermal autonomy is often limited, particularly during power outages or prolonged exposure to high ambient temperatures. This study explores the integration of phase change materials (PCMs) as a passive method of extending cold storage life. A transient thermal model and numerical simulations were developed to test the performance of different PCMs with melting temperatures between 25 and 30 °C and latent heat capacities of 150 to 260 kJ/kg, positioned in the inner walls of small refrigerators with volumes ranging from 20 to 125 L. The results indicate an increase in thermal autonomy of 45 to 120%, depending on the mass and location of the MCP, as well as a significant reduction in internal temperature fluctuations. The proposed approach offers robust and energy-efficient solutions for portable cold storage and passive refrigeration applications.

1 Introduction

Phase change materials (PCMs) are a class of substances capable of absorbing or releasing large amounts of latent heat during phase transitions, such as melting or solidification [1, 2]. Their ability to store thermal energy and passively regulate temperature makes them promising potential solutions for improving the energy efficiency of refrigeration systems. In small-scale refrigeration applications (such as portable coolers, mini domestic refrigerators and medical cooling units), PCMs offer an alternative to traditional cooling methods, which are often energy-intensive and use refrigerants that are harmful to the environment. This study investigates the integration of MCPs into these devices, focusing on their operating mechanisms, the technical challenges encountered, and their potential benefits in terms of reducing energy consumption and environmental impact. Through an analysis of recent experimental and numerical studies, we demonstrate how MCPs can transform the design of small refrigeration systems, thereby contributing to a transition towards more sustainable and efficient cooling technologies. Cheng et al. [3] studied the integration of phase change materials (PCMs) into the condenser of a standard domestic refrigerator, exploiting the material's ability to store heat during condensation and release it when the compressor stops.

* Corresponding author: salam.abdodhl@gmail.com

Xiaong et al. [4] proposed a hybrid refrigeration system combining compression and PCM storage to improve the energy efficiency of installations with high cooling demands, such as data centres and telecommunications units. Mohand et al. [5] applied a layer of PCM (approximately 10 mm thick) to the surface of a conventional refrigerator evaporator, observing a gain of approximately 2 °C in evaporation temperature compared to a bare evaporator. Mingzhu et al. [6] integrated PCMs into a cold storage system with the aim of recovering lost thermal energy and reusing it, thereby demonstrating improved energy efficiency. Eduard et al. [7] conducted experimental and numerical studies showing that the incorporation of PCMs significantly slows down the internal temperature rise in portable coolers. Omid et al. [8] numerically studied the effect of PCM thickness in a freezer compartment containing a eutectic PCM (NaCl–H_2O, melting at ~ 21°C), proving that performance increases with thickness. Shanhu et al. [9] demonstrated the feasibility of a 'passive' container based on phase change material (PCM), achieving effective cooling times of up to approximately 94.6 hours for combined road and rail transport. Nadiya et al. [10] developed an optimised eutectic mixture of PCM (lauric alcohol and cetyl alcohol, 80:20) for cold storage, with an adequate melting temperature (approximately 20 °C), high latent heat capacity (approximately 191.6 J/g), good thermal conductivity and improved cyclic stability.

The originality of this study lies in its examination of the combined effects of melting point and thickness of the phase change material (PCM) layer on the thermal performance of portable coolers. Unlike previous studies, which often focused on adjusting the mass of PCM, this research examines how varying the thickness of PCM affects melting/solidification kinetics, cold retention time, and internal thermal comfort. This approach allows the PFM thickness to be optimised according to the specific thermal profile of the application, highlighting adaptive cooler designs incorporating PFM for greater energy efficiency and performance. This work represents the initial results of a preliminary study on a simple case of this type of application in refrigeration.

2 Mathematical and numerical models

2.1 Physical model

The physical system, illustrated in Fig. 1, consists of a two-dimensional square cavity (50 cm × 50 cm) filled with air and in contact with a 1 cm thick Plexiglas plate. A layer of phase change material (PCM) is positioned along the left side of the cavity. The top, bottom and right surfaces are adiabatic, while the left surface is maintained at a constant temperature of 30 °C, which is chosen as the average temperature in Morocco.

The thermophysical properties of all materials used in this study are listed in Table 1. The main objective of this work is to study the influence of the melting temperatures of two paraffin-based PCMs (RT18HC and RT28HC). RT28HC paraffin was chosen for its melting point close to the average temperature of the region, while RT18HC paraffin was chosen to compare the effect of melting on the duration of cold retention) and the thickness of the MCP layer on the performance of the system, evaluated in terms of average air temperature (T_{avg}) and liquid fraction.

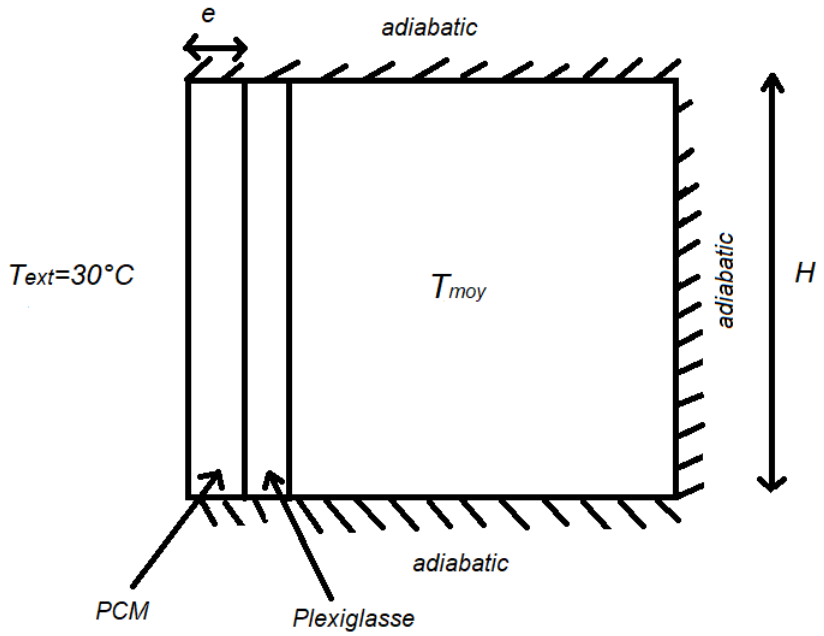

Fig. 1. Physical model.

Table 1. Thermo-physical properties of the used materials [11, 12].

	ρ, kg/m^3	k, W/m · K	c_p, J/kg · K	L, J/kg	μ, Pa · s	β, 1/K	T_m, °C
Plexiglas	1180	0,19	1470	-	-	-	-
RT28HC	770	0,2	2000	250000	0,00374	0,0005	28
RT18HC	880	0,2	2000	260000	0,00374	0,0005	18
Air	1,225	0,0242	1006,43	-	$1{,}79.10^{-5}$	0,0033	-

2.2 Governing equations

The basic equations are established on the basis of the following assumptions: (i) the problem is two-dimensional and transient; (ii) the flow of molten paraffin is laminar; (iii) liquid paraffin is considered to be an incompressible and Newtonian fluid; (iv) volume variations in the MCP during phase transition are neglected; (v) the Boussinesq approximation is used to take into account buoyancy effects due to density variations in the liquid MCP; (vi) the air flow inside the cavity is turbulent, mainly induced by buoyancy forces, and modelled using the standard k-ε turbulence model, as implemented in ANSYS Fluent 19.2; (vii) all materials (air, Plexiglas, and MCP) are assumed to be isotropic and homogeneous; (viii) the thermophysical properties of all materials are considered constant throughout the process.

The equations governing the conservation of mass, momentum, and energy to describe the flow behavior of molten paraffin are as follows:

Continuity equation

$$\nabla \mathbf{u_f} = 0 \tag{1}$$

Momentum equation

$$\rho_{\mathrm{f}}\left(\frac{\partial \mathbf{u_f}}{\partial t} + (\mathbf{u_f} \cdot \nabla)\boldsymbol{u_f}\right) = -\nabla p_{\mathrm{f}} + \mu_{\mathrm{f}}\nabla^2 \mathbf{u_f} + S_{\mathrm{M}} \tag{2}$$

$$S_{\mathrm{M}} = \rho_{\mathrm{f}}\,\mathbf{g}\,\beta(T_{\mathrm{f}} - T_{\mathrm{ref}}) - \frac{(1-f)^2}{f^3 + 10^{-3}} C_{\mathrm{mush}}\mathbf{u_f} \tag{3}$$

Energy equation

$$\left(\rho c_{\mathrm{p}}\right)_{\mathrm{f}}\left(\frac{\partial T_{\mathrm{f}}}{\partial t} + \mathbf{u_f} \cdot \nabla T_{\mathrm{f}}\right) = k_{\mathrm{f}}\nabla^2 T_{\mathrm{f}} - \rho_{\mathrm{f}} L \frac{\partial f}{\partial t} \tag{4}$$

where ρ_{f}, $\mathbf{u}_{\mathrm{f}}$, p_{f}, μ_{f}, f and β denote the density, velocity vector, pressure, dynamic viscosity, liquid fraction and thermal expansion coefficient of molten paraffin, respectively; T_{f} and T_{ref} represent the local and reference temperatures of paraffin. The term $(\rho c_p)_{\mathrm{f}}$ corresponds to the volumetric heat capacity of paraffin, and L is its latent heat.

Energy equation for solid (i.e., plexiglas)

$$\left(\rho c_{\mathrm{p}}\right)_{\mathrm{s}} \frac{\partial T_{\mathrm{s}}}{\partial t} = k_{\mathrm{s}}\nabla^2 T_{\mathrm{s}} \tag{5}$$

where $\left(\rho c_{\mathrm{p}}\right)_{\mathrm{s}}$, k_{s}, and T_{s} are the volumetric heat capacity, thermal conductivity, and local temperature in the solid, respectively.

2.3 Initial and boundary conditions

- Initial conditions:
$$f = 0, u = v = 0, T = T_{moy\ initial} = 5\ ℃ \tag{6}$$
- Left side of the system:
$$T = T_{ext} \ = 30\ ℃ \tag{7}$$
- Bottom, top, and right sides: adiabatic, i.e.,
$$\frac{\partial T}{\partial n} = 0, n \perp \text{wall} \tag{8}$$
- Non-slip condition at PCM-wall interface,
$$u = v = 0 \tag{9}$$

2.4 Numerical method

The computational domain, illustrated in Fig. 1, is discretised using a two-dimensional structured mesh to ensure accurate resolution of the flow and thermal fields. The equations of conservation of mass, momentum and energy are discretised using the finite volume method (FVM). Second-order schemes are applied for spatial and temporal discretisation to improve accuracy. Pressure-velocity coupling is handled by the PISO algorithm, and sub-relaxation factors are applied to improve convergence stability. The air flow inside the cavity is considered turbulent, mainly induced by buoyancy forces, and is modelled using the standard k-ε turbulence model available in ANSYS Fluent 19.2. Simulations are performed in double precision mode to minimise numerical errors. Convergence is ensured by verifying that the residuals of the continuity, momentum, energy and turbulence equations fall below 10-6, while all key physical variables, including temperature, velocity and turbulence quantities, exhibit stable behaviour at each time step.

2.5 Model validation

The numerical results obtained in this work are validated by comparison with the experimental data of Kamkari and Amlashi [13], as illustrated in Fig. 2. The same vertical rectangular cavity (120 × 50 mm²) as that used in ref. [13] is adopted here, with lauric acid as the phase change material (PCM), whose melting range is between 43.5 and 48.2 °C. A constant temperature of 70 °C is applied to the right wall. Overall, the comparison shows good agreement between the current model and the experimental observations of Kamkari and Amlashi [13]. The maximum deviation in total melting time remains limited to 1.6%.

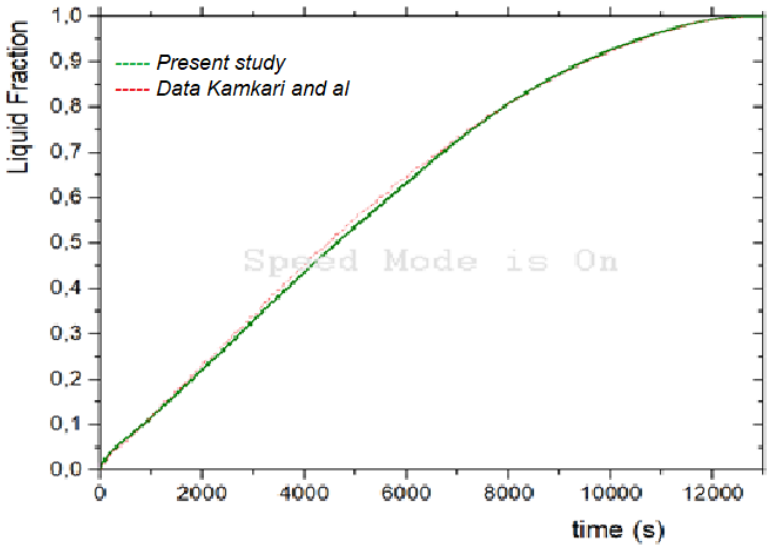

Fig. 2. Quantitative validation of our numerical model with the experimental results of Kamkari and Amlashi [10] in terms of liquid fraction.

3 Results and discussion

3.1 Effect of PCM melting point

In this section, the impact of the MCP melting temperature on the thermal behaviour of the system is analysed in terms of average air temperature and liquid fraction, as illustrated in Figs. 3 and 4. The main objective is to keep the internal air temperature as low as possible for extended periods. The results clearly indicate that the incorporation of MCP is beneficial, as it significantly reduces the air temperature. Furthermore, an MCP with a lower melting point, such as RT18HC, fails to maintain low air temperatures due to its rapid melting, as illustrated in Fig. 4. In contrast, the PCM with a melting point of 28°C (RT28HC) offers the best performance, effectively preventing air temperature rise over long periods and exhibiting a more gradual melting process, as shown in Figs. 3 and 4.

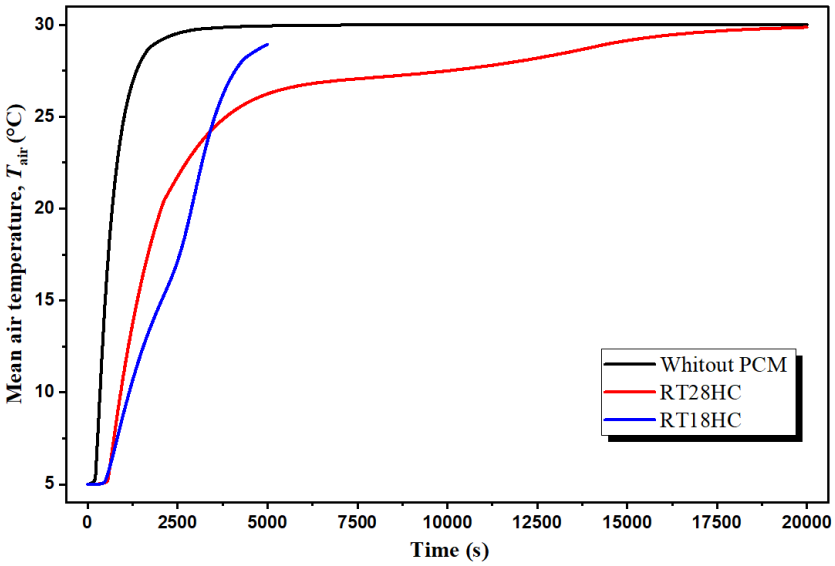

Fig. 3. Effect of PCM melting point on T_{moy}.

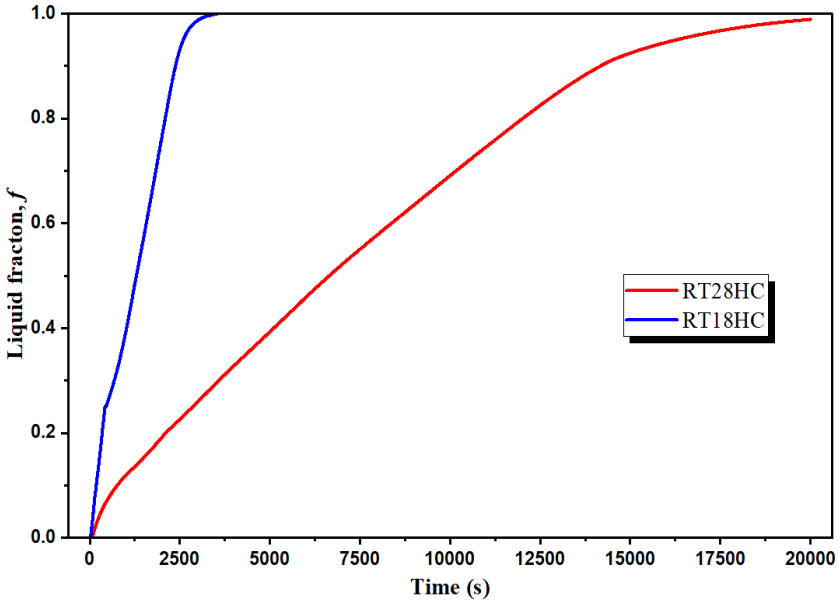

Fig. 4. Effect of PCM melting point on f.

3.2 Effect of PCM layer thickness

In this section, the influence of the MCP layer thickness (1 cm, 2 cm, 3 cm and 4 cm) on the thermal behaviour of the system is analysed in terms of average air temperature and liquid fraction, as illustrated in Figs. 5 and 6.

Fig. 5 shows the temporal evolution of the average air temperature for different PCM layer thicknesses. The results indicate that increasing the PCM thickness from 1 cm to 4 cm effectively reduces the average air temperature inside the cavity. This effect may be related to the increased thermal resistance of thicker PCM layers, which slows down the penetration of heat from the external environment. In addition, the relatively low thermal conductivity of PCM further limits heat transfer to the layer, resulting in a more gradual and controlled melting process. Consequently, thicker PCM layers act as a more effective thermal buffer, delaying the rise in air temperature. Fig. 6 shows the corresponding evolution of the liquid fraction of PCM over time. The results demonstrate that as the thickness of the PCM increases, the melting rate decreases significantly. It appears that increasing the thickness of the PCM layer from 1 cm to 4 cm reduces the liquid fraction almost exponentially. This behaviour is physically consistent because a thicker PCM layer increases the thermal diffusion path, slowing down the propagation of the heat front and distributing the absorbed energy over a larger volume. As a result, the melting process is prolonged, thus improving the thermal regulation capacity of the system.

In summary, these results highlight the crucial role of the thickness of the phase change material (PCM) in regulating the internal air temperature and controlling the kinetics of phase change. Optimising the thickness of the PCM layer enables better energy storage, more consistent temperature profiles and prolonged cold retention, all of which are essential for improving the performance of small refrigeration systems and portable cooling devices.

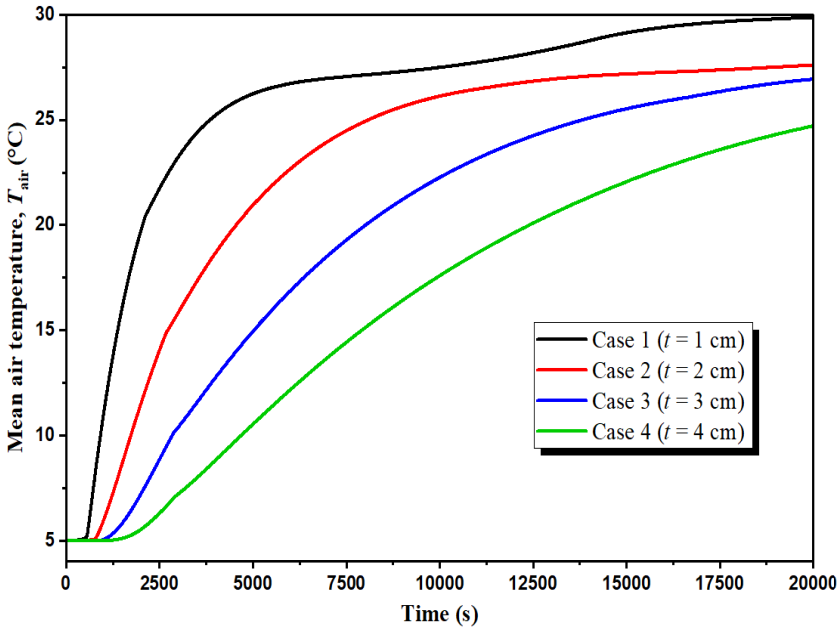

Fig. 5. Effect of PCM layer thickness on T_{moy}.

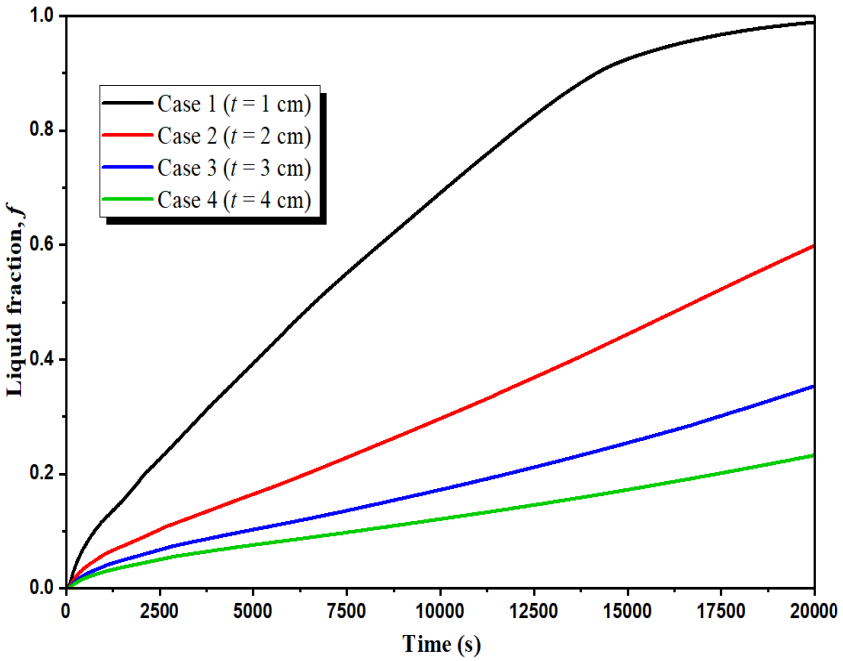

Fig. 6. Effect of PCM layer thickness on f.

4 Conclusion

The integration of phase change materials (PCMs) into a cooling system highlights their considerable potential for improving thermal performance as well as sustainability and environmental protection. The results show a direct relationship between the thickness of the PCM and the cooling time. According to Figs. 5 and 6, the temperature is reduced by nearly 20% and the liquid fraction is approximately 80%. This is because the thickness of the PCM determines the total amount of latent energy it can store during phase change. The greater the thickness, the greater the available mass of PCM and the greater the heat absorbed by the PCM, thus preventing the internal temperature from exceeding the desired threshold. Logically, this results in a longer cooling time. Fig. 4 shows that choosing a suitable MCP with a melting/solidification point close to the temperature of the region gives good results in terms of cold retention time. To refine this relationship, experimental testing and analysis of the thermophysical properties of the MCP (conductivity, latent heat, transition temperature) would confirm the observed trends and determine the optimal thickness for each application.

References

1. M. Errebii, F.Z. Laktaoui Amine, Y. El Alami, A. Chaabi, A. Mourid, M. El Alami, Y. Yao, Synergistic enhancement and stabilization of thermoelectric generator (TEG) performance using finned metal foam–PCM composites. Energy **348**, 140538 (2026). https://doi.org/10.1016/j.energy.2026.140538
2. M. Errebii, A. Mourid, A. Charraou, M. El Alami, M. Kriraa, Performance optimization of a thermoelectric generator using metal foam/phase change material composites and fins. Energy **334**, 137806 (2025). https://doi.org/10.1016/j.energy.2025.137806

3. W.-L. Cheng, B.-J. Mei, Y.-N. Liu, Y.-H. Huang, X.-D. Yuan, A novel household refrigerator with shape-stabilized PCM (Phase Change Material) heat storage condensers: An experimental investigation. Energy **36**, 5797–5804 (2011). https://doi.org/10.1016/j.energy.2011.08.050
4. X. Chen, Q. Zhang, Z. J. Zhai, D. Wu, S. Liao, Experimental study on operation characteristics of a novel refrigeration system using phase change material. Energy Build. **150**, 516–526 (2017). https://doi.org/10.1016/j.enbuild.2017.05.069
5. M. Berdja, A. Hamid, O. Sari, Characteristics and thickness effect of phase change material and frost on heat transfer and thermal performance of conventional refrigerator: Theoretical and experimental investigation. Int. J. Refrig. **97**, 108–123 (2019). https://doi.org/10.1016/j.ijrefrig.2018.10.003
6. M. Xia, Y. Yuan, X. Zhao, X. Cao, Z. Tang, Cold storage condensation heat recovery system with a novel composite phase change material. Appl. Energy **175**, 259–268 (2016). https://doi.org/10.1016/j.apenergy.2016.05.001
7. E. Oró, L. F. Cabeza, M. M. Farid, Experimental and numerical analysis of a chilly bin incorporating phase change material. Appl. Therm. Eng. **58**, 61–67 (2013). https://doi.org/10.1016/j.applthermaleng.2013.04.014
8. O. Ghahramani Zarajabad R. Ahmadi, Numerical investigation of different PCM volume on cold thermal energy storage system. J. Energy Storage **17**, 515–524 (2018). https://doi.org/10.1016/j.est.2018.04.013
9. S. Tong, B. Nie, Z. Li, C. Li, B. Zou, L. Jiang, Y. Jin, Y. Ding, A phase change material (PCM) based passively cooled container for integrated road-rail cold chain transportation – An experimental study. Appl. Ther. Eng. **195**, 117204 (2021). https://doi.org/10.1016/j.applthermaleng.2021.117204
10. N. Philip, G. Raam Dheep, A. Sreekumar, Cold thermal energy storage with lauryl alcohol and cetyl alcohol eutectic mixture: Thermophysical studies and experimental investigation. J. Energy Storage **27**, 101060 (2020). https://doi.org/10.1016/j.est.2019.101060
11. Plexiglas XT: https://www.plexiglas.de/files/plexiglas-content/pdf/technische-informationen/211-1-FR-PLEXIGLAS-GS-XT.pdf
12. RT28HC and RT18HC: https://www.rubitherm.eu/en/productcategory/organische-pcm-rt.
13. B. Kamkari, H. J. Amlashi, Numerical simulation and experimental verification of constrained melting of phase change material in inclined rectangular enclosures. Int. J. Heat Mass Transfer **88**, 211–219 (2017). https://doi.org/10.1016/j.icheatmasstransfer.2017.07.023